DESIGN AND BEAM DYNAMICS STUDY OF DISK-LOADED STRUCTURE FOR MUON LINAC

K. Sumi*, T. Iijima, K. Inami, Y. Sue, M. Yotsuzuka,

Nagoya University, Nagoya, Aichi, Japan

H. Ego, M. Otani, N. Saito, T. Mibe, M. Yoshida,

High Energy Accelerator Research Organization (KEK), Tsukuba, Ibaraki, Japan

Y. Kondo, K. Moriya, Japan Atomic Energy Agency (JAEA), Tokai, Naka, Ibaraki, Japan

Y. Takeuchi, Kyushu University, Fukuoka, Japan

Y. Nakazawa, Ibaraki University, Mito, Ibaraki, Japan

H. Yasuda, University of Tokyo, Tokyo, Japan

Abstract

The disk-loaded structures (DLS) in the muon LINAC are under development for the J-PARC muon g−2/EDM experiment. Four DLSs with an accelerating gradient of 20 MV/m take charge of muon acceleration from 40 MeV to 212 MeV, which corresponds to 70% to 94% of the speed of light. The quasi-constant gradient type TM01-2π/3 mode DLSs with gradually varying disk spacing was designed and it was confirmed that the cumulative phase slip due to the mismatch between muon and phase velocity can be suppressed to less than 2 degrees at the frequency of 2592 MHz. In addition, the optimum synchronous phase and the lattice were investigated to satisfy the requirements of the total emittance less than 1.5π mm mrad and the momentum spread less than 0.1% in RMS.

INTRODUCTION

The world experimental average value of the muon anomalous magnetic moment, g−2, deviates from the standard model prediction by 4.2 times the standard deviation [1]. This discrepancy may be a sign of new physics beyond the standard model. The muon electric dipole moment, EDM, which is unobserved, could also be enhanced if new physics exists.

The experiment in J-PARC plans to validate the discrepancy of muon g−2 and to search muon EDM with novel techniques: low emittance muon beam, compact storage magnet, no electrostatic focusing, and three-dimensional spiral injection [2]. The low emittance muon beam is generated by thermalized muonium ionization followed by their acceleration by the muon LINAC. The requirements for beam quality are low transverse normalized emittance of approximately 1.5π mm mrad and momentum of 300 MeV/c with a small spread of less than 0.1% in root-mean-square (RMS).

The muon linac consists of four kinds of structures: radio frequency quadrupole (RFQ), inter-digital H-mode drift-tube linac (IH-DTL), disk and washer coupled cavity linacs (DAW-CCL), and disk-loaded traveling wave structures (DLS), matching the varying muon velocity for the short-time — sufficiently shorter than the muon lifetime of

2.2 μs — acceleration to suppress decay loss. The DLS section consists of four DLSs approximately 2 m in length and takes charge of acceleration from 40 MeV to 212 MeV in kinetic energy, corresponding velocity range of 70-94% of the speed of light. The transport line includes two quadrupole magnets between each DLS. The requirement for the DLS is a high accelerating gradient of 20 MV/m.

STRUCTURE DESIGN

Since DLS is an accelerating structure that has been in use for relativistic electron acceleration and has proven to have a sufficiently high gradient, we apply it for high-velocity muon acceleration. The essential feature of DLS for muon acceleration, different from DLS for electron acceleration, is that disk spacing (cell length) varies proportionally to muon velocity [3]. Since assuming a constant gradient is convenient for the velocity calculation of muon through the DLS section, a quasi-constant gradient type with linear tapering iris apertures is adopted.

Table 1: Parameters of the First Cell in the DLS Section of Two Different Frequencies

Parameters	L-band [5]	S-band
Structure type	disk-loaded traveling wave quas-constant gradient type	
Resonant mode	TM01-2π/3	
Frequency [MHz]	1296	2592
Muon velocity ($\beta = v/c$)	0.695	
Cell length (D) [mm]	53.698	26.885
Iris aperture ($2a$) [mm]	43.370	25.875
Cylinder diameter ($2b$) [mm]	181.147	92.070
Disk thickness [mm]	5.000	
Quality factor (Q)	17116	11289
Shunt impedance (Z) [MOhm/m]	29.15	31.16
Group velocity (v_g/c) [%]	1.22	1.52
Field attenuation factor (α) [/m]	0.0648	0.163
Cell accelerating gradient (E_{acc}) [MV/m/MW$^{1/2}$]	1.94	3.13

---

* ksumi@hepl.phys.nagoya-u.ac.jp

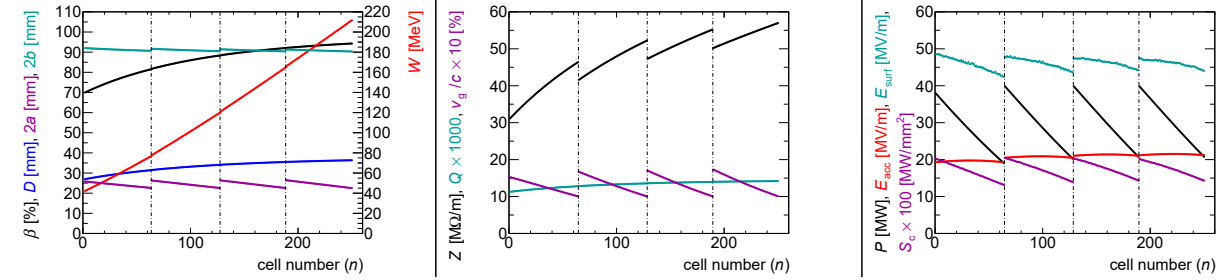This is a preprint — the final version is published with IOP

Figure 1: The S-band DLS cell parameters; first DLS (n=1-64), second DLS (n=65-128), third DLS (n=129-189) and fourth DLS (n=190-250).

An operating frequency is one of the most important parameters in an accelerating structure design. Therefore, we consider two different operating frequencies and summarize the parameters of two types of DLS calculated using SUPERFISH [4] in Table 1. At first, the L-band DLS was designed with an operating frequency of 1296 MHz, the same frequency as DAW-CCL, to ensure longitudinal acceptance. However, this structure required excessive RF power compared with L-band klystron power of 40 MW to obtain an accelerating gradient of 20 MV/m [5]. Therefore, the S-band DLS with twice the operating frequency is designed for higher efficiency and shows its accelerating gradient is approximately 60% higher than the L-band DLS with the same power. A narrower iris aperture results in a higher accelerating gradient, but the current iris aperture of each DLS is determined so that group velocity is faster than $1\%c$ to ensure sufficient coupling strength for field stability [5].

For the above consideration, we select S-band and design four DLSs with the synchronous phase (ϕ_s) of −13 degrees, determined based on the discussion in the next section. The designed and calculated cell parameters are plotted in Fig. 1. Some parameter symbols are as in Table 1 and others are the kinetic energy (W), the RF power (P), the peak surface electric field (E_{surf}), and the modified Poynting vector (S_c) [6]. W is calculated assuming the constant energy gain per unit length:

$$\Delta W = e\overline{E_{acc}} \cos \phi_s, \quad (1)$$

where $\overline{E_{acc}}$ is the average of E_{acc} for each DLS: 19.6, 20.8, 21.3, and 21.4 MV/m. β is naturally obtained by W. Since we choose $2\pi/3$ mode, the cell length is determined as:

$$D = \beta\lambda/3, \quad (2)$$

where λ = 115.661 mm is the wavelength of 2592 MHz RF. $2a$ is optimized by iterative calculation with the different taper angle until E_{acc} at the first and last cells become the same. After optimization, the distribution of E_{acc} is arched and the difference of E_{acc}, defined as $(\max(E_{acc}) − \min(E_{acc}))/\overline{E_{acc}}$, is approximately 2% for all DLSs. $2b$ is adjusted to have a resonant frequency of 2592 MHz for each cell. Z and Q depend on D, and v_g depends on $2a$. The RF power of DLS1 is 38 MW which is tuned to obtain a 300 MeV/c muon beam at the end of the DLS section. The power dissipation is calculated considering a 3% deterioration of Q. E_{surf} and S_c are evaluated as

the criteria for accelerating field stability in the situation of 40 (or 38) MW flat-top RF input at a pulse length of 1 μs. Since the Kilpatrick limit [7] at 2592 MHz is 43.8 MV/m, the bravery factor is within the range from 0.97 to 1.11. S_c is sufficiently below the safety threshold of 5 MW/mm^2 [6] at a pulse length of 200 ns.

BEAM DYNAMICS SIMULATION

The longitudinal acceptance depends on ϕ_s. An approximate separatrix at the entrance of the DLS section is shown in Fig. 2, where assuming $\overline{E_{acc}}$ = 20 MV/m, ϕ_s = −13 degrees, and no velocity change. The contour plot in Fig. 2 shows the simulated beam distribution after acceleration through DAW-CCL. The ratio of the loss particles, out of the separatrix, are estimated to be approximately 0.6% of the total. Although a larger acceptance is desirable considering the possibility of the emittance growth due to the beam mismatch upstream, a larger $|\phi_s|$ results in a smaller energy gain and a larger transverse RF defocusing force.
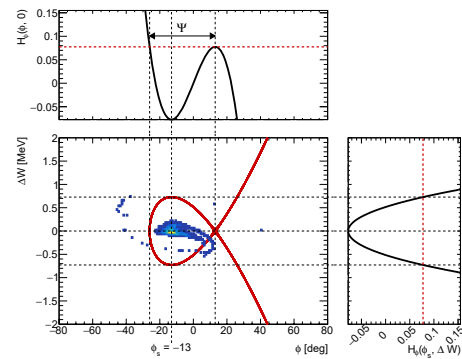

Figure 2: The longitudinal beam distribution including the separatrix and the Hamiltonian H_ϕ.

An average RF defocusing force per cell is described by the approximate formula

$$F_x(x) = -\frac{\pi}{\beta\gamma^2}\frac{x}{\lambda}eE_{acc}\sin\phi_s = -m_\mu c^2\beta^2\gamma K_1 x, \quad (3)$$

where x is the horizontal distance from the beam axis, m_μ is the muon mass, γ is the relativistic factor, and K_1 is the quadrupole focusing strength. The lattice function of the first DLS and its downstream transport line is defined as shown

in Fig. 3. The field strength of each quadrupole magnet is optimized considering the Twiss-beta function. We conduct the parameter scan by the horizontal/vertical phase advance ($\sigma_{x/y}$) and find the optimum lattice whose maximum Twiss-beta in the first DLS is minimum under the condition that the phase advance is less than 80 degrees considering the possibility of beam instability. The gradient of each quadrupole magnet is approximately 20 T/m. The Twiss-beta functions of the optimized lattice under periodic boundary conditions are plotted in Fig. 3.
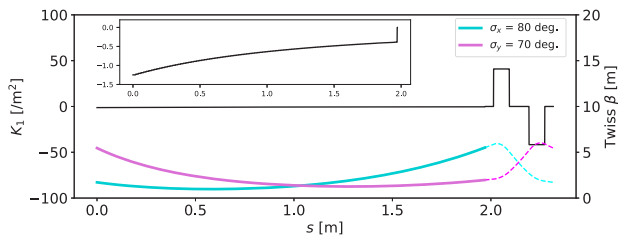
Figure 3: The lattice function of the first DLS section and two quadrupole magnets and the Twiss-beta function under periodic boundary conditions.

The particle tracking simulation is conducted using GPT [8]. As a first step, the simulation with a reference muon is performed to validate the phase slip. Due to the quasi-constant gradient, the difference between actual and ideal energy gain causes a phase slip. The large phase slip can result in large beam loss because of narrow longitudinal acceptance. The cell phase slip is defined as $\Delta\phi = \varphi_{\text{beam}} - \varphi_{\text{RF}}$, where φ_{beam} corresponds to the time beam takes to fly per cell, and $\varphi_{\text{RF}} = 120$ degrees is ideal RF phase advance per cell. $\Delta\phi$ and the cumulative phase slip are evaluated by ideal muon tracking as shown in Fig. 4. In the actual machine, it is estimated that the phase slip of a few degrees to φ_{RF} occurs due to frequency error caused by machining error. Therefore, compared to the phase slip due to machining error, the $\Delta\phi$ of up to 1.5 degrees is sufficiently suppressed.

Then, the particle tracking simulation is conducted using realistic beam distribution estimated from the upstream accelerator simulation. The accelerated beam distributions are shown in Fig. 5. The momentum spread is 0.07% in RMS and is sufficiently small. Figure 6 shows the beam envelope and the transverse emittance through the DLS section. The envelope is enough smaller than DLS apertures and the normalized RMS emittance does not grow during acceleration thanks to beam matching at the entrance of the DLS section using the initial condition obtained in Fig. 3. The transmission rate is 99.4%, and all beam loss is due to longitudinal acceptance.

SUMMARY AND PROSPECTS

We discussed the operating frequency, the synchronous phase, and the lattice of the DLS section for muon acceleration. The designed S-band DLS is simulated to accelerate the muon beam with sufficient accelerating gradient without
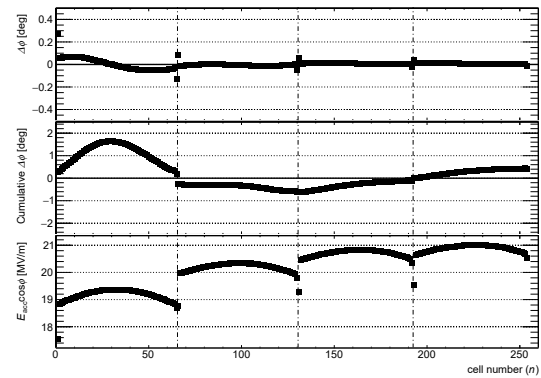

Figure 4: The cell phase slip (top), the cumulative phase slip (middle), and the average electric field which affects the ideal muon.
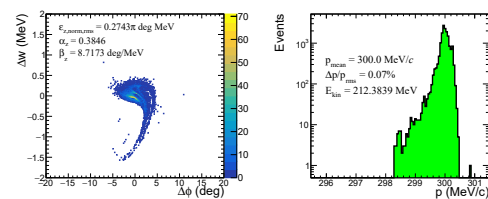

Figure 5: The longitudinal beam distributions at the exit of the DLS section.
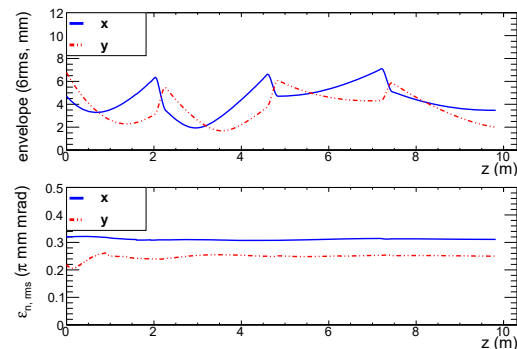

Figure 6: The beam envelope of six RMS (top) and the transverse normalized RMS emittance through the DLS section.

large phase slip and to satisfy the requirements for momentum spread and emittance. We are now designing the coupler cell and will fabricate the first and last regular cells and two coupler cells to evaluate actual parameters and to demonstrate the tuning method.

ACKNOWLEDGMENTS

REFERENCES

[1] B. Abi *et al.*, "Measurement of the positive muon anomalous magnetic moment to 0.46 ppm", *Phys. Rev. Lett.*, vol. 126, p. 141801, 2021. `doi:10.1103/PhysRevLett.126.141801`

[2] M. Abe *et al.*, "A new approach for measuring the muon anomalous magnetic moment and electric dipole moment", *Prog. Theor. Exp. Phys.*, vol. 2019, p. 053c02, 2019. `doi:10.1093/ptep/ptz030`

[3] Y. Kondo *et al.*, "Beam dynamics design of the muon linac high beta section", *J. Phys.: Conf. Ser.*, vol. 874, p. 012054, 2017. `doi:10.1088/1742-6596/874/1/012054`

[4] J. H. Billen and L. M. Young, "Poisson Superfish", LA-UR-96-1834, 1996.

[5] K. Sumi *et al.*, "Basic design of L-band disk-loaded structure for muon Linac", *in Proc. 18th Annu. Meet. PASJ (PASJ2021)*, Aug. 2021, pp. 133-137.

[6] A. Grudiev *et al.*, "New local field quantity describing the high gradient limit of accelerating structures", *Phys. Rev. Spec. Top. Accel. Beams*, vol. 12, p. 102001, 2009. `doi:10.1103/PhysRevSTAB.12.102001`

[7] W. D. Kilpatrick, "A criterion for vacuum sparking designed to include both R.F. and D.C.", University of California Radiation Laboratory Report No. UCRL-2321, 1953.

[8] Pulser Physics, "General Particle Tracer", `http://www.pulsar.nl/gpt/`

This is a preprint — the final version is published with IOP